JOURNAL OF THE MECHANICAL BEHAVIOR OF BIOMEDICAL MATERIALS 15 (2012) 103–111

Available online at www.sciencedirect.com

SciVerse ScienceDirect

www.elsevier.com/locate/jmbbm

Research Paper

Tribology and hydrophobicity of a biocompatible GPTMS/PFPE coating on Ti6Al4V surfaces

*Bharat Panjwani, Sujeet.K. Sinha**

Department of Mechanical Engineering, National University of Singapore, 9 Engineering Drive 1, 117576 Singapore, Singapore

ARTICLE INFO

Article history:
Received 15 March 2012
Received in revised form
22 June 2012
Accepted 26 June 2012
Available online 24 July 2012

ABSTRACT

Tribological properties of perfluoropolyether (PFPE) coated 3-glycidoxypropyltrimethoxy silane (GPTMS) SAMs (self-assembled monolayers) onto Ti6Al4V alloy substrate were studied using ball-on-disk experiments. GPTMS SAMs deposition onto a Ti6Al4V alloy surface was carried out using solution phase method. Ultra-thin layer of PFPE was dip-coated onto SAMs modified specimens. Tribological tests were carried out at 0.2 N normal load and rotational speed of 200 rpm using track radius of 2 mm. Wear track and counterface surface conditions were investigated using optical microscopy. PFPE modified specimens were baked at 150 °C for 1 h to investigate the effect of thermal treatment on tribological properties. Surface characterization tests such as contact angle measurement, AFM morphology and X-ray photoelectron spectroscopy were carried out for differently modified specimens. PFPE overcoat meets the requirements of cytotoxicity test using the ISO 10993-5 elution method. PFPE top layer lowered the coefficient of friction and increased wear durability for different specimens (with and without GPTMS intermediate layer). PFPE overcoat onto GPTMS showed significant increase in the wear resistance compared with overcoat onto bare Ti6Al4V specimens. The observed improvement in the tribological properties can be attributed to the change in the interaction of PFPE molecules with the substrate surface due to the GPTMS intermediate layer.

1. Introduction

Titanium and its alloys find applications in many biomedical and industrial devices due to their high specific strength, corrosion resistance and biocompatibility. Titanium has also been proposed as a suitable MEMS (Micro-electro-mechanical systems) structural material for its physical and mechanical properties (Aimi et al., 2004). Titanium alloys are potential structural materials for MEMS devices in biomedical applications due to their excellent biocompatibility. However, poor tribological properties of titanium alloys can limit their applications in MEMS devices (Budinski, 1991; Yildiz et al., 2009).

To improve the tribological properties of titanium alloys, various surface treatments and coatings have been proposed. Plasma nitriding is one of the widely used surface treatments for titanium alloys (Molinari et al., 1997; Yildiz et al., 2008). Ceramic coatings have also been explored in earlier studies for improving the tribological properties of titanium alloys (Fei et al., 2009). Researchers have also explored polymer coatings to address the tribological limitations of titanium alloys (Panjwani et al., 2011).

*Corresponding author.
E-mail address: mpesks@nus.edu.sg (Sujeet.K. Sinha).

1751-6161/$ - see front matter © 2012 Elsevier Ltd. All rights reserved.
http://dx.doi.org/10.1016/j.jmbbm.2012.06.016

Some researchers have investigated surface modification of titanium alloys by the use of molecularly thin layers to address tribological limitations in MEMS applications (Sun and Zhang, 2008a,b). However, studies to improve tribological properties of titanium and titanium alloys for MEMS applications are limited. Thus, there is further need to investigate the use of molecularly thin layers to improve tribological properties of titanium alloys in MEMS applications.

Researchers have investigated SAMs (self-assembled monolayers) coatings to address the tribological limitations of titanium alloys for MEMS applications (Sun and Zhang, 2008a,b). Even though some SAMs exhibit a low coefficient of friction, wear resistance of these monomolecular layers is not adequate to obtain a long life in the high velocity moving MEMS components. Lack of molecular flexibility and mobility of SAMs cause poor wear durability and low load capacity of coatings (Ren et al., 2002b; Rye et al., 1997; Sung et al., 2003). Therefore, some researchers have investigated the use of a mobile portion as a top layer which can provide self-reparability due to the migration of mobile molecules into the sliding contact resulting into high wear resistance. This concept has been explored for hard disk lubrication (Katano et al., 2003). Use of PFPE as a top layer has been investigated in different studies to improve wear durability of SAMs (Satyanarayana and Sinha, 2005; Satyanaryana et al., 2007).

The current study investigates the use of an ultra-thin molecular layer of PFPE overcoat onto GPTMS SAM (3-glycidoxypropyltrimethoxy silane self-assembled monolayer with epoxy terminal group) to address tribological limitations of titanium alloys. GPTMS SAM is reactive towards chemical groups such as amine ($–NH_2$), acid (–COOH), hydroxyl (–OH) and methoxy ($–OCH_3$) due to the presence of epoxy terminal group (Ellis, 1993). Ti6Al4V is a most widely used titanium alloy (Donachie, 2000) and has been used as substrate material in this study.

GPTMS SAMs deposition onto Ti6Al4V substrate was carried out using solution phase method. Prior to SAMs coating, oxygen plasma treatment was carried out to facilitate hydroxylization of the substrate surface (Yoshinari et al., 2006). PFPE top layer was coated using dip-coating method onto GPTMS modified as well as bare Ti6Al4V alloy specimens. To carry out heat treatment, PFPE coated specimens were baked at 150 °C for 1 h. Tribological characterizations were carried out in a ball-on-disk tribometer employing counterface of Si_3N_4 ball (4 mm dia.). Tests were conducted at 0.2 N normal load and 200 RPM speed using track radius of 2 mm. Physical characterizations (contact angle measurement and atomic force microscope imaging) and chemical characterization (X-ray photoelectron spectroscopy) were carried out for different surface modified specimens. Cytotoxicity evaluation of PFPE top layer was carried out using the ISO 10993-5 elution method. PFPE was chosen due to its chemical and thermal stability as well as good lubricity (Liu and Bhushan, 2003) and it has shown improved tribological characteristics as a top ultra-thin layer onto SAMs in earlier studies (Satyanarayana and Sinha, 2005; Satyanaryana et al., 2007). Wear track and counterface surface conditions were investigated to infer the underlying friction and wear mechanisms.

2. Experimental methodology

2.1. Materials

Ti6Al4V-ELI Grade 5 (as per ASTM B265) specimens having dimensions of 25 mm × 25 mm × 5 mm were used as substrate. 3-Glycidoxypropyltrimethoxysilane (CH_2–O–CH–-CH_2–O–$(CH2)_3$–Si–$(OCH_3)_3$) (procured from Aldrich) was used for the preparation of SAM solution. A commercial PFPE (molecular weight 4000 g/mol, with OH terminal groups at both ends, monodispersed) having chemical formula $(OH–CH_2–CF_2–(O–CF_2–CF_2)_p–(O–CF_2)_q–O–CF_2–CH_2–OH$, where p, q are integers and p/q ratio is 2/3) was procured from Solvay Solexis, Singapore. Hydrofluoropolyether solvent (H-Galden ZV) ($HCF_2O–(CF_2O)_p–(CF_2CF_2O)_q–CF_2H$, ratio p/q is 2/3), obtained from Ausimont Inc., was used as the solvent for the preparation of PFPE solution. Toluene (99.5% anhydrous), ethanol (99.8%), acetone and distilled water were also used for the preparation of the SAMs.

2.2. Specimens preparation procedure

Titanium alloy samples were surface-ground using SiC abrasive papers of 160, 320, 800 and 1000 grit sizes successively. The direction of grinding was changed by 90 degrees between successive grit sizes. After grinding, samples were polished on a polishing wheel using diamond paste of grain size 1 μm followed by 0.25 μm. Afterward, samples were cleaned sequentially using acetone, ethanol and distilled water in an ultrasonic bath each for the duration of 15 min and dried with N_2 gas. Resulting surface roughness (rms) of Ti6Al4V specimens (after grinding, polishing and cleaning) was 11.4–12.3 nm (measured by AFM in a representative scan area of 5 μm × 5 μm).

Ti6Al4V alloy specimens (after grinding, polishing and cleaning) were oxygen-plasma treated for 10 min in Harrick Plasma Cleaner using RF power supply of 18 W. Plasma treated Ti6Al4V alloy specimens were immersed into the epoxy SAM solution (using toluene as the solvent) at a concentration of 1 vol% and left for 18 h. Afterward, the modified samples were washed with toluene and ethanol to remove any physisorbed SAM molecules. Finally, samples were blow-dried with N_2 gas. Samples were kept in a desiccator until further characterizations. The GPTMS deposition procedure is similar to that reported in an earlier study (Luzinov et al., 2000) except that, in this study, the procedure was carried at 25 °C and a relative humidity of ~70%.

PFPE was coated onto GPTMS SAM-modified Ti6Al4V alloy substrates using a custom-built dip-coating machine. The SAM-modified Ti6Al4V alloy substrates were dipped into the PFPE solution (0.5 wt% PFPE solution in H-Galden solvent) and held for 1 min. Dipping and withdrawn procedures were carried out at a constant speed of 2.1 mm/s. Similarly, bare Ti6Al4V alloy samples, after oxygen-plasma treatment, were also coated with PFPE. For the thermal treatment, PFPE coated samples were baked at 150 °C for 1 h. All specimens were stored in desiccator until further surface characterizations.

2.3. Depositional characterization and surface analysis

Static water contact angle measurement was used to evaluate hydrophilic or hydrophobic nature of the prepared specimen surfaces. Water contact angle measurements are used to assess surface free energy of surfaces. Surface free energy is one of the important characteristics which affect tribological properties of surfaces. VCA Optima Contact Angle System (AST Products, Inc. USA) was used to measure static water contact angle. Distilled water droplets with a volume of 0.5 μl were used for the measurements. To arrive at an average and standard deviation of contact angle measurements for different modifications, data were collected for three different samples at five different locations on each sample.

Topographic (roughness) measurement of the specimen surfaces was carried out using Atomic force microscope (Dimension 3000 AFM, Digital Instruments, USA). Images were scanned in air using a monolithic silicon tip in the tapping mode. In measurements, set point voltage of 1–2 V and scan rate of 0.5 Hz were used.

XPS (Thermo Fisher Scientific Theta Probe) was used to study the chemical state of the surface material.

2.4. Tribological characterization

UMT-2 (Universal Micro Tribometer, CETR, USA) was used for tribological tests in a ball-on-disk mode under dry conditions. A Si_3N_4 ball of 4 mm diameter was used as the counterface with a roughness of 5 nm (roughness value provided by supplier). The ball was cleaned using acetone before each test. Si_3N_4 ball was used as the counterface since Si_3N_4 material has much higher hardness when compared to that of Ti6Al4V alloy and is inert towards organic species.

The spindle rotational speed of 200 rpm was used for different tests in tribological characterizations. This spindle rotational speed gives a sliding speed of 41.9 mm/s at used track diameter of 4 mm. Applied normal load was 0.2 N for all the tests. Tribological tests were carried out in a class 100 clean booth environment having a temperature of 25 ± 2 °C and a relative humidity of 55 ± 5%.

The wear life for the tribological tests was taken as the number of life cycles after which the coefficient of friction exceeded 0.3 or a visible wear mark/track appeared on the substrate, whichever occurred earlier (Miyoshi, 2001). Optical microscope ($\times100$) was used to observe the worn track surfaces after appropriate number of sliding cycles to infer wear mechanism.

2.5. Biocompatibility test

The cytotoxicity test was carried out by NAMSA (Northwood, OH, USA). This test was done according to the guidelines of "International Organization for Standardization 10993-5: Biological Evaluation of Medical Devices, Part 5: Tests for In Vitro Cytotoxicity". Before cytotoxicity testing, specimens were sterilized using ethylene oxide and degassed. Fifteen specimens were used for cytotoxicity testing by ISO elution method-1 × MEM extract method.

In a single preparation, test specimens were extracted in single strength minimum essential medium (1 × MEM) at a temperature of 37 °C for the time duration of 24 h. The negative control, reagent control and positive control were also prepared as per the requirements mentioned in the testing standards. Triplicate monolayers of L-929 mouse fibroblast were dosed with prepared extracts. Incubation was carried out at a temperature of 37 °C in the presence of 5% CO_2 for the time duration of 48 h. Following the incubation, the triplicate monolayers were microscopically (100 magnification) examined for any abnormal cell morphology and cellular degeneration.

3. Results and discussion

3.1. Water contact angle results

After polishing, cleaning and drying processes, bare Ti6Al4V alloy surface showed a water contact angle value of $73\pm4^\circ$. In an earlier study (Wang et al., 1997), water contact angle of 72° was observed that is within the range of water contact angles measured in this study. After 10 min of oxygen plasma treatment of Ti6Al4V alloy surface, water contact angle was reduced to $6\pm1^\circ$. This is due to the hydrophilic nature of Ti6Al4V alloy surface after oxygen plasma exposure indicating increased surface energy. Oxide layers generated by oxygen plasma method exhibit reduced stiction for hydrocarbon contaminations (Aronsson et al., 1997). Oxygen plasma treatment also hydroxylizes Ti surface which facilitates covalent attachment of SAMs (Yoshinari et al., 2006).

GPTMS coating onto oxygen plasma treated Ti6Al4V alloy exhibited a water contact angle value of $60\pm2^\circ$ which is in good agreement with the value of 62° reported in an earlier study (Elender et al., 1996). PFPE overcoat onto GPTMS modified Ti6Al4V alloy showed a water contact angle of $90\pm5^\circ$. After heat treatment, water contact angle value of the Ti6Al4V/GPTMS/PFPE specimen was increased to $112\pm6^\circ$.

PFPE coating onto oxygen plasma treated Ti6Al4V alloy surface exhibited a water contact value of $52\pm3^\circ$. After heat treatment, PFPE coating onto Ti6Al4V alloy surface showed increased water contact angle value of $110\pm2^\circ$. Table 1 summarizes the water contact angle values (average and standard deviation) for different specimen types prepared in this study.

Observed increase in the water contact angle value of PFPE top layers, after heat treatment, is due to the reduction in the available surface hydroxyl groups (Tao and Bhushan, 2005). Low surface energy is one of the desirable properties for MEMS coatings since high surface energy leads to stiction

Table 1 – Measured water contact angle values for different specimen types.

Specimen type	Water contact angle (°)
Ti6Al4V	73 ± 4
Ti6Al4V (after O_2 plasma treatment)	6 ± 1
Ti6Al4V/GPTMS	60 ± 2
Ti6Al4V/GPTMS/PFPE	90 ± 5
Ti6Al4V/GPTMS/PFPE (heat treated)	112 ± 6
Ti6Al4V/PFPE	52 ± 3
Ti6Al4V/PFPE (heat treated)	110 ± 2

resulting in the failure of components. Low surface energy of the coatings suggests their potential applications in preventing or reducing stiction and friction arising due to the surface and capillary forces (Mastrangelo, 1997).

3.2. AFM morphology

Bare Ti6Al4V alloy specimen surface (after polishing, grinding and cleaning) showed the surface roughness (rms) of 11.8 nm as measured by AFM imaging using the scan area of 5 μm × 5 μm. Scratches created in the polishing process can be observed in AFM morphology image (Fig. 1(a)). Bare Ti6Al4V with PFPE overcoat exhibited the surface roughness (rms) of 1.7 nm. PFPE overcoat onto Ti6Al4V, after heat treatment, showed the surface roughness (rms) of 1.2 nm.

GPTMS coating deposited onto Ti6Al4V showed the surface roughness (rms) of 6.8 nm. PFPE overcoat onto GPTMS coating exhibited the surface roughness (rms) of 2.5 nm. After heat treatment, PFPE coating onto GPTMS showed the surface roughness (rms) of 5.0 nm. Fig. 1 shows AFM images of representative specimen types prepared in this study.

Thickness of GPTMS SAMs coating obtained in an earlier study utilizing similar deposition method as followed in the present study was reported to be close to 0.95 nm (Luzinov et al., 2000). Thickness of PFPE overcoat deposited using similar dip-coating procedure followed in the present study was reported to be close to 2–3 nm in an earlier research (Eapen et al., 2002). No thickness measurements of GPTMS SAMs coating and PFPE overcoat were carried out in this study due to difficulties arising from higher surface roughness (11.8 nm) of Ti6Al4V alloy substrate in comparison with estimated thicknesses of deposited coatings. As observed in the AFM imaging results, GPTMS coating has reduced the surface roughness of the substrate. Observed significant change in the surface roughness also suggests the possibility of GPTMS forming as a multi-layer rather than monolayer probably due to high humidity ambient conditions (Luzinov et al., 2000; Satyanaryana et al., 2007). PFPE overcoat onto different specimens also resulted in significant reduction of surface roughness value which can be attributed to the possibility of linear and flexible PFPE molecules filling-up the surface texture features such as valleys.

3.3. XPS analysis

Wide scan XPS spectra of Ti6Al4V/GPTMS specimen showed strong C1s, O1s and Ti2p peaks as shown in Fig. 2. Due to nanometer thickness of the deposited GPTMS SAMs coating, substrate is also detected in XPS spectra. Fig. 3 shows the comparison of C1s peaks of Ti6Al4V/GPTMS and Ti6Al4V specimens. High resolution XPS spectrum of C1s scan for Ti6Al4V/GPTMS specimen showed two strong peaks. Peak at 284.6 eV represents (C–C) bonds and 286.4 eV corresponds to the (C–O) bonds in the epoxy SAM molecules. These two strong peaks are indicative of epoxy SAM presence as seen in earlier studies (Cloarec et al., 2002; Wong and Krull, 2005). In comparison with GPTMS, Ti6Al4V alloy surface showed only one C1s peak. Observed change in the XPS core-level spectra of C1s for Ti6Al4V/GPTMS specimen in comparison with that of Ti6Al4V specimen indicates the successful deposition of GPTMS SAM coating.

F1s spectra of Ti6Al4V/PFPE and Ti6Al4V/GPTMS/PFPE specimens (with and without heat treatment) have been shown in Fig. 4 indicating the presence of PFPE molecules on specimens after dip-coating.

3.4. Tribological results

Bare Ti6Al4V alloy and surface modified Ti6Al4V alloy specimens' tribological properties were evaluated using Si_3N_4 as the counterface in a ball-on-disk tribometer. Table 2 tabulates steady-state friction coefficient (evaluated at the end of 600 sliding cycles) values of specimens investigated in this study. Fig. 5 summarizes the wear life (average and standard

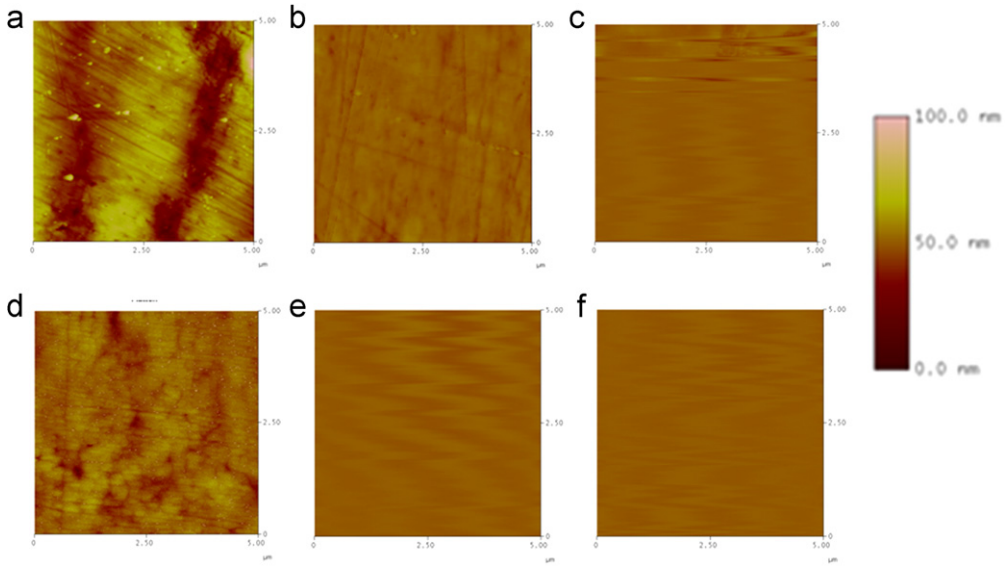

Fig. 1 – AFM imaging (scan area: 5 μm × 5 μm, vertical scale: 100 nm). (a) Ti6Al4V, (b) Ti6Al4V/PFPE, (c) Ti6Al4V/PFPE (heat treated), (d) Ti6Al4V/GPTMS, (e) Ti6Al4V/GPTMS/PFPE and (f) Ti6Al4V/GPTMS/PFPE (heat treated).

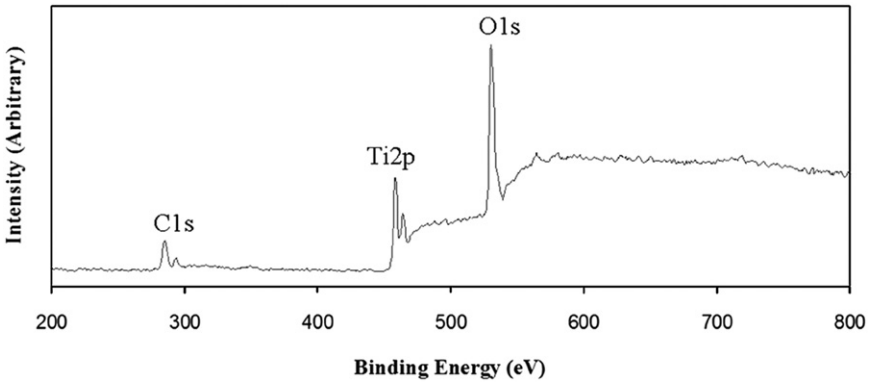

Fig. 2 – Wide scan XPS spectra of Ti6Al4V/GPTMS specimen.

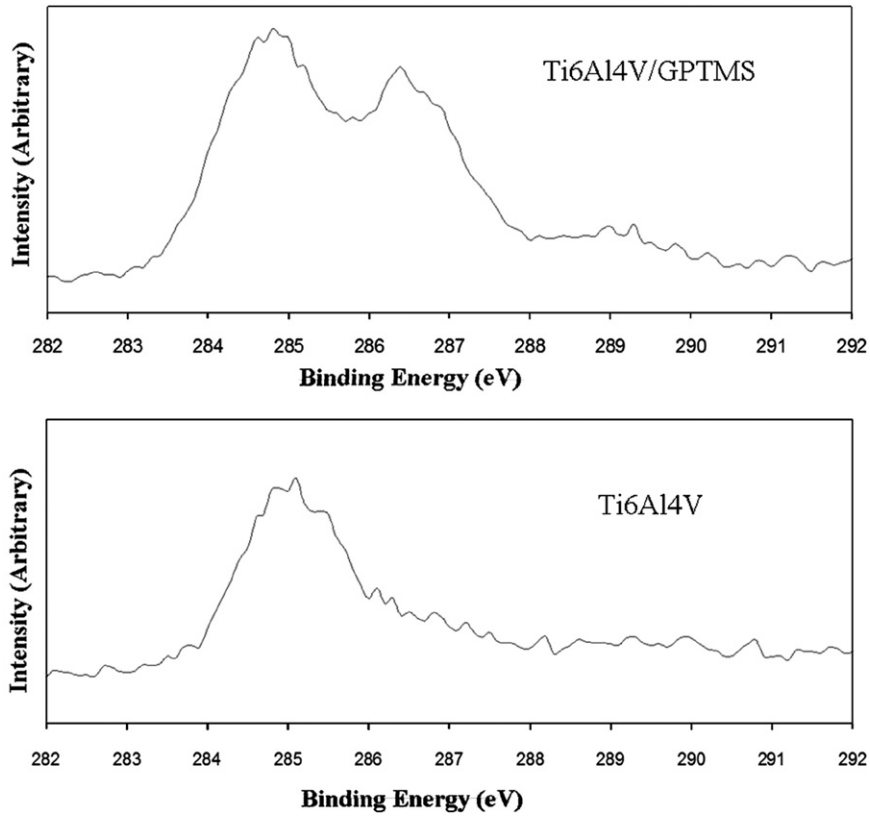

Fig. 3 – Comparison of C1s high resolution XPS scan for Ti6Al4V/GPTMS and Ti6Al4V specimens.

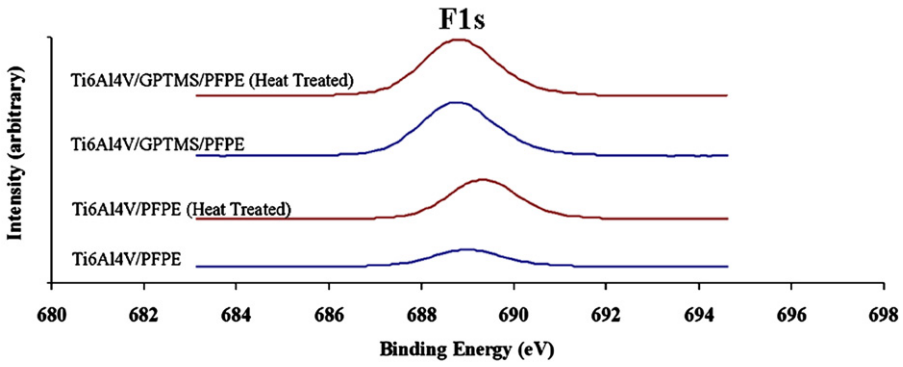

Fig. 4 – Intensities of F1s peaks for Ti6Al4V/PFPE and Ti6Al4V/GPTMS/PFPE specimens in high resolution XPS scan.

deviation) of prepared specimens (six specimens tested for each treatment) in this study. Error bars represent standard deviation for tested specimens. Bare Ti6Al4V alloy and GPTMS deposited Ti6Al4V specimens showed wear life of less than 100 sliding cycles for tested conditions (not shown in Fig. 5). Wear durability data of samples from each specimen type were collected from minimum six different samples using three different tracks on each sample.

Fig. 6 shows the variation in the coefficient of friction vs. sliding cycles for a representative PFPE coated Ti6Al4V alloy specimen. For comparison, results of the tribological characterization of bare Ti6Al4V alloy have also been tabulated for the same testing conditions. Bare Ti6Al4V alloy specimens showed high coefficient of friction (0.5–0.6) as shown in Fig. 6 and Table 2. High surface energy and mechanical instability of oxide layer result into poor tribological properties of bare Ti6Al4V alloy (Budinski, 1991; Yildiz et al., 2009). PFPE modified Ti6Al4V alloy (with and without heat treatment) specimens have showed lower coefficient of friction and specimens after heat treatment exhibited lower wear durability in comparison with specimens without heat treatment (see Figs. 5 and 6). Reduction in the wear durability can be attributed to the reduction in the mobile portion of PFPE overcoat after heat treatment. Reduction in the wear durability after heat treatment of PFPE coating has been observed in an earlier study onto a different substrate (Miyake et al., 2006).

Fig. 7 shows the variation in the coefficient of friction with sliding cycles for a representative PFPE coated Ti6Al4V/GPTMS specimen. Similar tribological test results have also been tabulated for Ti6Al4V/GPTMS specimen. For Ti6Al4V/GPTMS/PFPE specimen shown in Fig. 7, coating failure was not observed for a test duration of 100,000 sliding cycles.

Table 2 – Summary of coefficients of friction for tested specimens.

Specimen type	Steady-state coefficient of friction
Ti6AL4V	0.5–0.6
Ti6AL4V/PFPE	0.12–0.13
Ti6AL4V/PFPE (heat treated)	0.11–0.12
Ti6AL4V/GPTMS	0.5–0.6
Ti6AL4V/GPTMS/PFPE	0.11–0.12
Ti6AL4V/GPTMS/PFPE(heat treated)	0.12–0.13

Epoxy SAMs (GPTMS) modified Ti6Al4V alloy exhibited high coefficient of friction (0.5–0.6) at the tested condition of 0.2 N normal load and 200 rpm (see Table 2 and Fig. 7). Observed tribological properties of epoxy SAMs modified substrate are similar to the observation in an earlier study (Sidorenko et al., 2002). PFPE overcoat onto epoxy-SAM modified Ti6Al4V alloy (with and without heat treatment) reduced coefficient of friction and increased the wear durability (see Figs. 5 and 7). Epoxy-SAMs modified Ti6Al4V alloy specimens with PFPE overcoat showed high wear durability (90,700 ± 13,900 sliding

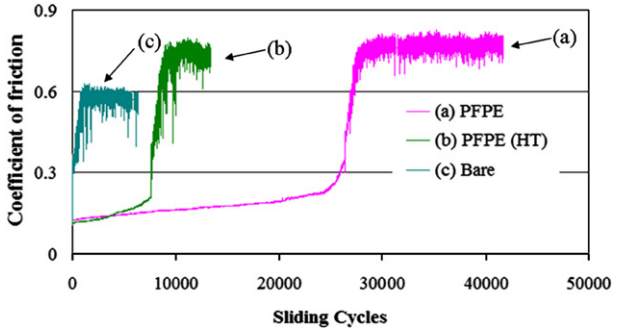

Fig. 6 – Variation of friction coefficient as a function of the sliding cycles using Si_3N_4 ball as the counterface (track radius: 2 mm, normal load: 0.2 N, spindle speed: 200 rpm). (a) Ti6AL4V/PFPE, (b) Ti6AL4V/PFPE (heat treated) and (c) Ti6Al4V.

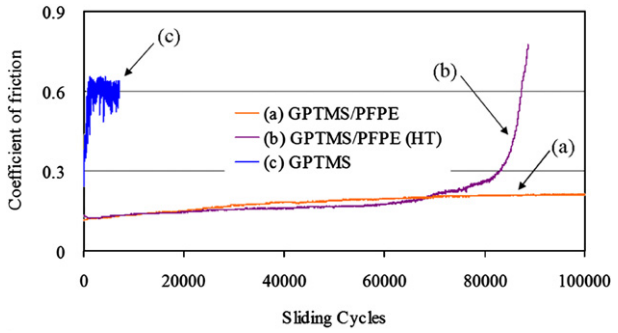

Fig. 7 – Variation of friction coefficient as a function of the sliding cycles using Si_3N_4 ball as the counterface (track radius: 2 mm, normal load: 0.2 N, spindle speed: 200 rpm). (a) Ti6AL4V/GPTMS/PFPE, (b) Ti6AL4V/GPTMS/PFPE (heat treated) and (c) Ti6Al4V/GPTMS.

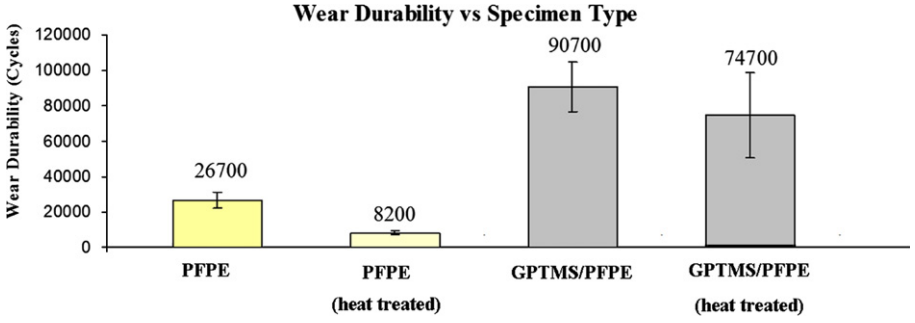

Fig. 5 – Wear durability (number of sliding cycles before failure) of different coatings tested in the study onto Ti6Al4V substrate.

cycles) although heat treatment has resulted into some reduction in the wear durability (74,700±24,000 sliding cycles).

PFPE overcoat (with and without heat treatment) on Ti6Al4V alloy and GPTMS SAMs modified alloy has reduced the coefficient of friction to 0.11–0.13 for different specimens investigated in this study as observed in Table 2.

Fig. 8(a) and (b) shows the optical micrographs of the wear track and counterface surface after completion of 5000 cycles of the sliding test for bare Ti6Al4V specimen. There was extensive wear debris accumulation around the track (Fig. 8(a)) and counterface surface of Si_3N_4 ball showed severe damage (Fig. 8(b)). Roughness (rms) of wear track shown in Fig. 8(a) was 87.8 nm (measured by AFM in a representative scan area of 5 μm × 5 μm; AFM picture not shown). Similar wear track and counterface conditions were observed for GPTMS deposited Ti6Al4V specimens after completion of 5000 sliding cycles (Fig. 8(c) and (d)).

Fig. 9 shows the wear track and counterface surface after completion of 100,000 sliding cycles using the coating of GPTMS/PFPE onto Ti6Al4V alloy for one of the sliding test where coating had not failed. As seen in Fig. 9(a), no wear debris was observed around wear track although mild scratch was formed by the impression of the counterface. There was a little material transfer to the counterface of Si_3N_4 ball (see Fig. 9(b)). After cleaning with acetone, counterface showed smooth surface with no signs of damage as observed in Fig. 9(c).

As observed in different tribological tests, mild scratching on the wear track without the presence of wear debris and smooth counterface surface accompanied by little material transfer were observed before the failure of the film. After the failure of the film, extensive wear debris accumulation along the wear track and worn counterface surface were noticed.

PFPE coating onto bare Ti6Al4V alloy as well as GPTMS SAMs deposited Ti6Al4V alloy has resulted into the lowering of friction coefficient and increase in the wear durability. This can be attributed to lower surface energy (Makkonen, 2004) as well as flexible and mobile nature of PFPE molecules (Mate, 1992) resulting into a low resistance in the shearing at the sliding interface.

PFPE overcoat onto GPTMS coated Ti6Al4V alloy can consist of three parts as speculated in earlier studies (Satyanarayana and Sinha, 2005; Satyanaryana et al., 2007). PFPE top layer can consist of molecules trapped in surface texture, strongly adsorbed portion and the mobile portion. Strongly adsorbed portion results due to strong physical adsorption and covalent bonding as well as hydrogen bonding interaction. During the initial sliding cycles, mobile as well as bonded portion of PFPE will lubricate the contact region. After partly squeezing of the mobile portion of PFPE, lubrication will be supported by the bonded portion of PFPE molecules. After complete removal of the mobile and bonded portion of PFPE due to shearing and frictional heating, high friction and wear will be followed leading to the failure of the coating.

High wear resistance of Ti6Al4V/GPTMS/PFPE specimens compared with Ti6Al4V/PFPE specimens can result from the possible interaction of PFPE molecules (having hydroxyl group) with GPTMS (having epoxy group) intermediate layer. Chemical interaction of hydroxyl group with epoxy group resulting into ether linkage has been reported in previous research studies (Elender et al., 1996; Ellis, 1993). Bonding of PFPE molecules with substrate surface can result into a high wear resistance due to the retention of PFPE molecules for longer duration at the sliding surface. It has been observed in some studies that dual-lubricant layer combination consisting of initially bonded layer having strong-polar top group

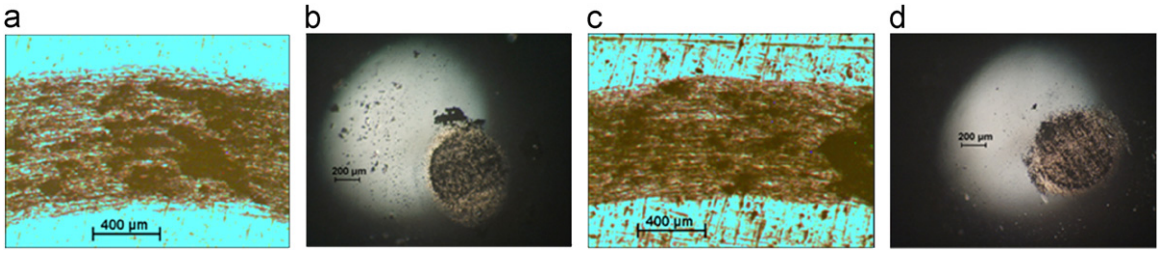

Fig. 8 – Optical micrographs of wear track and counterface surface after completion of 5000 sliding cycles. The scale bar is 400 μm in the images (a) & (c) and is 200 μm in the images (b) & (d). (a) Wear track (Ti6Al4V specimen), (b) counterface surface (Ti6Al4V specimen), (c) wear track (Ti6Al4V/GPTMS specimen) and (d) counterface surface (Ti6Al4V/GPTMS specimen).

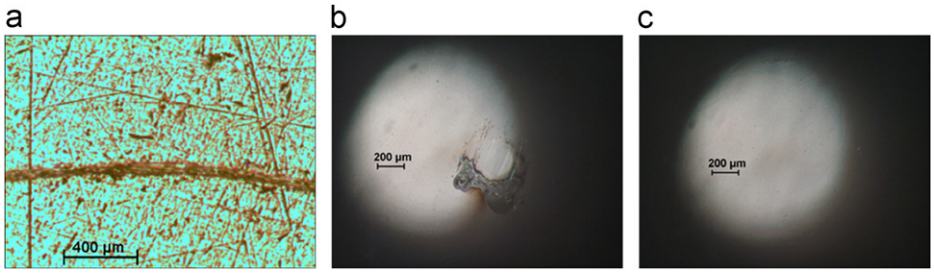

Fig. 9 – Optical micrographs of Ti6Al4V/GPTMS/PFPE specimen's wear track and counterface surface after completion of 100,000 sliding cycles. The scale bar is 400 μm in the image (a) and is 200 μm in the images (b) & (c). (a) Wear track, (b) counterface surface and (c) counterface surface after cleaning.

with top mobile layer having weaker polar group shows improved tribological properties in comparison with the use of only any one of the monolayers (Katano et al., 2003).

3.5. *Cytotoxicity test results*

ISO 10993 recommends a set of tests to determine the biocompatibility of a material depending on factors such as application area, contact duration and manner of contact. However, cytotoxicity test has been used as a preliminary test to assess the biocompatibility of a material in biomedical applications due to its relevance to all implant applications. This test identifies the cytotoxic potential of leachables extracted from test specimens.

Studies evaluating bio-compatibility of GPTMS have been documented in earlier research works. In one of the study, noncytotoxicity of GPTMS was validated by the assessment of cytocompatibility of hybrids of gelatin–GPTMS and chitosan–GPTMS in an in-vitro study (Ren et al., 2002a). In another study, biocompatibility of GPTMS SAM was confirmed using both bacterial culture (E.coli DH5α, Gram negative bacteria) and plant tissue culture (wheat seed) (Kumar et al., 2011).

Biocompatibility of PFPE polymer has been examined by researchers and long-term biocompatibility of PFPE has been validated in different studies for biomedical applications (Sweeney et al., 2008; Xie et al., 2006).

In the present study, H-Gladen ZV60 was used as the solvent for PFPE. To confirm that it has not affected the biocompatibility of PFPE, PFPE top layer, coated onto a polymer film, was tested for cytotoxicity using ISO elution method-1 × MEM extract method. In cytotoxicity testing carried out using PFPE overcoat, no cytotoxicity effects such as cell lysis were seen in any of the test wells during the microscopic examinations. No change in the pH value was noticed after the test duration of 48 h.

Grade of the test results should be less than 2 (mild reactivity) to meet the requirements of the ISO elution method-1 × MEM extract. Based upon test analysis results, it was inferred that PFPE top layer exhibited cytotoxicity level of grade 0 (reactivity: none) according to the test guidelines, thus PFPE top layer coating meets the requirements of the ISO elution method-1 × MEM extract.

In view of the mentioned previous research studies and cytotoxicity test carried out in the present study, noncytotoxic nature of GPTMS and PFPE coatings are validated. It indicates the biocompatible nature of the composite coating of GPTMS/PFPE investigated in this study.

3.6. *Potential applications of GPTMS/PFPE coating*

GPTMS/PFPE coating exhibits hydrophobicity, noncytotoxicity and excellent tribological properties (low friction and high wear durability). Hydrophobic coatings exhibit low surface energy. Lower friction and water-repellent nature of the hydrophobic coatings are useful in different biomedical applications having contact surfaces in relative motion. Low surface energy of biomedical coatings has been found to be useful in bio-film inhibition for few in-vivo applications (Roosjen et al., 2006). Coatings on metallic stent having low surface energy and noncytotoxic nature are beneficial in improving the biocompatibility of metal surface with body fluids by inhibiting the release of cytotoxic extracts from the metal surface into the body environment (Pendyala et al., 2009). Thus, the obtained composite coating of GPTMS/PFPE can find different applications in biomedical devices. Due to the molecularly low thickness of this coating, it can be particularly useful in biomedical MEMS applications where thickness of the surface coating is a crucial consideration for its usage.

4. Conclusions

In this study, the potential of the molecularly thin GPTMS/PFPE coating to address the tribological limitations of titanium alloys has been evaluated. Physical characterizations (contact angle measurement, AFM imaging), chemical characterization (XPS) and tribological tests were carried out for the obtained specimen coatings. From the results and observations of this study, following important conclusions can be drawn.

1. PFPE overcoat onto GPTMS deposited Ti6Al4V alloy exhibits improved tribological properties such as low coefficient of friction (0.11–0.13) and high wear durability.
2. Wear resistance of PFPE overcoat on GPTMS deposited Ti6Al4V alloy is significantly higher (90,700 ± 13,900 sliding cycles) than PFPE overcoat without GPTMS deposition (26,700 ± 4,900) which can be attributed to the increased bonding of PFPE with the substrate due to the GPTMS intermediate layer.
3. PFPE overcoat also reduces surface roughness of the substrate due to filling-up of surface texture by this nano-lubricant.
4. Low coefficient of friction, high wear resistance, hydrophobicity and noncytotoxic nature of the coating are suitable characteristics for their potential applications in biomedical instruments. Due to the molecularly low thickness, GPTMS/PFPE coating is particularly suitable for biomedical MEMS applications.

Acknowledgments

This research is supported by the Singapore National Research Foundation under its CRP (Competitive Research Program) funding (Award Number: NRF-CRP 2–2007-04). The views expressed herein are those of the authors and are not necessarily those of the Singapore National Research Foundation.

REFERENCES

Aimi, M.F., Rao, M.P., Macdonald, N.C., Zuruzi, A.S., Bothman, D.P., 2004. High-aspect-ratio bulk micromachining of titanium. Nature Materials 3, 103–105.

Aronsson, B.O., Lausmaa, J., Kasemo, B., 1997. Glow discharge plasma treatment for surface cleaning and modification of metallic biomaterials. Journal of Biomedical Materials Research 35, 49–73.

Budinski, K.G., 1991. Tribological properties of titanium alloys. Wear 151, 203–217.

Cloarec, J.P., Deligianis, N., Martin, J.R., Lawrence, I., Souteyrand, E., Polychronakos, C., Lawrence, M.F., 2002. Immobilization of homooligonucleotide probe layers onto Si/SiO_2 substrates: characterization by electrochemical impedance measurements and radiolabelling. Biosensors & Bioelectronics 17, 405–412.

Donachie, M.J., 2000. Titanium: a technical guide, second edition ASM International, Materials Park, OH.

Eapen, K.C., Patton, S.T., Zabinski, J.S., 2002. Lubrication of microelectromechanical systems (MEMS) using bound and mobile phases of Fomblin Zdol®. Tribology Letters 12, 35–41.

Elender, G., Kuhher, M., Sackmann, E., 1996. Functionalisation of Si/SiO_2 and glass surfaces with ultrathin dextran films and deposition of lipid bilayers. Biosensors & Bioelectronics 11, 565–577.

Ellis, B. (Ed.), 1993. Chemistry and Technology of Epoxy Resins. Bryan Ellis, Blackie Academic & Professional, New York 72–116.

Fei, C., Hai, Z., Chen, C., Yangjian, X., 2009. Study on the tribological performance of ceramic coatings on titanium alloy surfaces obtained through microarc oxidation. Progress in Organic Coatings 64, 264–267.

Katano, T., Oka, M., Nakazawa, S., Aramaki, T., Kusakawa, K., 2003. Characteristics of dual lubricant layers. IEEE Transactions on Magnetics 39, 2489–2491.

Kumar, S., Singh, J., Agrawal, V.V., Ahamad, M., Malhotra, B.D., 2011. Biocompatible self-assembled monolayer platform based on (3-glycidoxypropyl)trimethoxysilane for total cholesterol estimation. Analytical Methods 3, 2237–2245.

Liu, H., Bhushan, B., 2003. Nanotribological characterization of molecularly thick lubricant films for applications to MEMS/NEMS by AFM. Ultramicroscopy 97, 321–340.

Luzinov, I., Julthongpiput, D., Liebmann-Vinson, A., Cregger, T., Foster, M.D., Tsukruk, V.V., 2000. Epoxy-terminated self-assembled monolayers: molecular glues for polymer layers. Langmuir 16, 504–516.

Makkonen, L., 2004. Friction as a result of surface tension. 27th Annual Meeting of the Adhesion Society, Wilmington, NC, USA, pp. 399–401.

Mastrangelo, C.H., 1997. Adhesion-related failure mechanisms in micromechanical devices. Tribology Letter 3, 223–238.

Mate, C.M., 1992. Atomic-force-microscope study of polymer lubricants on silicon surfaces. Physical Review Letters 68, 3323–3326.

Miyake, S., Wang, M., Ninomiya, S., 2006. Nanotribological properties of perfluoropolyether-coated magnetic disk evaluated by vertical and lateral vibration wear tests. Surface & Coatings Technology 200, 6137–6154.

Miyoshi, K., 2001. Solid lubrication fundamentals and applications. Marcel Dekker, Inc..

Molinari, A., Strafellini, G., Tesi, B., Bacci, T., Pradelli, G., 1997. Effects of load and sliding speed on the tribological behaviour of Ti–6Al–4V plasma nitrided different temperatures. Wear 203, 447–545.

Panjwani, B., Satyanarayana, N., Sinha, S.K., 2011. Tribological characterization of a biocompatible thin film of UHMWPE on Ti6Al4V and the effects of PFPE as top lubricating layer. Journal of the Mechanical Behavior of Biomedical Materials 4, 953–996.

Pendyala, L., Jabara, R., Robinson, K., Chronos, N., 2009. Passive and active polymer coatings for intracoronary stents: novel devices to promote arterial healing. Journal of Interventional Cardiology 22, 37–48.

Ren, L., Tsuru, K., Hayakawa, S., Osaka, A., 2002a. Novel approach to fabricate porous gelatin-siloxane hybrids for bone tissue engineering. Biomaterials 23, 4765–4773.

Ren, S., Yang, S., Zhao, Y., Zhou, J., Xu, T., Liu, W., 2002b. Friction and wear studies of octadecyltrichlorosilane SAM on silicon. Tribology Letters 13, 233–239.

Roosjen, A., Norde, W., van der Mei, H.C., Busscher, H.J., 2006. The use of positively charged or low surface free energy coatings versus polymer brushes in controlling biofilm formation. Progress in Colloid and Polymer Science 132, 138–144.

Rye, R.R., Nelson, G.C., Dugger, M.T., 1997. Mechanistic aspects of alkylchlorosilane coupling reactions. Langmuir 13, 2965–2972.

Satyanarayana, N., Sinha, S.K., 2005. Tribology of PFPE overcoated self-assembled monolayers deposited on Si surface. Journal of Physics D: Applied Physics 38, 3512–3522.

Satyanaryana, N., Gosvami, N., Sinha, S.K., Srinivasan, M.P., 2007. Friction, adhesion and wear durability studies of ultra-thin PFPE overcoated 3-Glycidoxypropyltrimethoxy silane SAM on Si surface. Philosophical Magazine 87, 3209–3227.

Sidorenko, A., Ahn, H.S., Kim, D.I., Yang, H., Tsukruk, V.V., 2002. Wear stability of polymer nanocomposite coatings with trilayer architecture. Wear 252, 946–955.

Sun, C.G., Zhang, H.C., 2008a. Preparation and characterization of γ-aminopropyltrimethoxysilane and octadecyltrichlorosilane self-assembled monolayers on titanium films. Key Engineering Materials 373–374, 472–475.

Sun, C.G., Zhang, H.C., 2008b. Tribological properties of Ti6Al4V alloy by FOTS self-assembled monolayers modification treatment. Technical Sessions. In: Proceedings of CIST2008 & ITS-IFToMM2008 Beijing, China.

Sung, I-H., Yang, J-C., Kim, D-E., Shin, B-S., 2003. Micro/nanotribological characteristics of self-assembled monolayer and its application in nano-structure fabrication. Wear 255, 808–818.

Sweeney, D.F., Vannas, A., Hughes, T.C., Evans, M.D.M., McLean, K.M., Xie, R.Z., Pravin, V.K., Prakasam, R.K., 2008. Synthetic corneal inlays. Clinical and Experimental Optometry 91 (1), 56–66.

Tao, Z., Bhushan, B., 2005. Bonding, degradation, and environmental effects on novel perfluoropolyether lubricants. Wear 259, 1352–1361.

Wang, R., Hashimoto, K., Fujishima, A., Chikuni, M., Kojima, E., Kitamura, A., Shimohigoshi, M., Watanabe, T., 1997. Light-induced amphiphilic surfaces. Nature (London) 388, 431–432.

Wong, A.K.Y., Krull, U.J., 2005. Surface characterization of 3-glycidoxypropyltrimethoxysilane films on silicon-based substrates. Analytical and Bioanalytical Chemistry 383, 187–200.

Xie, R.Z., Evans, M.D.M., Bojarski, B., Hughes, T.C., Chan, G.Y., Nguyen, X., Wilkie, J.S., McLean, K.M., Vannas, A., Sweeney, D.F., 2006. Two-year preclinical testing of perfluoropolyether polymer as a corneal inlay. Investigative Ophthalmology & Visual Science 47, 574–581.

Yildiz, F., Yetim, A.F., Alsaran, A., Celik, A., 2008. Plasma nitriding behavior of Ti6Al4V orthopedic alloy. Surface & Coatings Technology 202, 2471–2476.

Yildiz, F., Yetim, A.F., Alsaran, A., Efeoglu, I., 2009. Wear and corrosion behaviour of various surface treated medical grade titanium alloy in bio-simulated environment. Wear 267, 695–701.

Yoshinari, M., Hayakawa, T., Matsuzaka, K., Inoue, T., Oda, Y., Shimono, M., Ide, T., Tanaka, T., 2006. Oxygen plasma surface modification enhances immobilization of simvastatin acid. Biomedical Research 27 (1), 29–36.